Available online at www.sciencedirect.com
ScienceDirect
Journal of Power Sources 174 (2007) 508–514
JOURNAL OF POWER SOURCES
www.elsevier.com/locate/jpowsour

Composite cathode structure/property relationships

S. Babinec [a,*], H. Tang [a], A. Talik [a], S. Hughes [a], G. Meyers [b]

[a] *Core New Products, The Dow Chemical Company, Midland, MI 48674, USA*
[b] *Core Analytical Sciences, The Dow Chemical Company, Midland, MI 48674, USA*

Available online 23 June 2007

Abstract

Battery-active materials are routinely evaluated via the electrochemical performance of their composite electrodes which are prepared with standard formulations and routine processing conditions. The relationship between electrochemical responses and formulation variables are not commonly explored, however, and mechanical properties are almost never considered. We therefore offer some quite basic studies of the effects of formulation on these properties for the most common Li-ion chemistry—$LiCoO_2$ particles with PVDF binders, focusing on the effects of porosity and microscopic structure.

Keywords: PVDF; $LiCoO_2$; C-rates; Young's modulus; Elastic modulus; TEM

1. Introduction: balancing electrochemistry and mechanics

Batteries are principally designed and optimized as electrochemical devices, with scarce attention devoted to their mechanical attributes. Consideration of the device life-cycle however reveals several potentially important issues associated with porous composite electrode manufacturing and use. We therefore offer some quite basic mechanical characterizations of composite electrodes, examining the constituent materials as dense composites and the porous electrode structures, both across a broad compositional range. Bulk and thin film analysis techniques are applied to samples created with standard research laboratory scale practices of the most common Li-ion chemistry—$LiCoO_2$ electroactive particles with PVDF binders and cyclic carbonate electrolytes. The electrochemical rate capabilities of the porous films are evaluated with standard button cell battery analysis. Mechanical characterizations include standard tests for bulk properties of dense composites as well-specialized analysis of the porous films. We will show that composite electrode designs which optimize mechanical durability and ruggedness degrade electrochemical performance, due to the need to optimize the porous electrode structure for Li^+ transport.

1.1. Composite design constraints

Polymers are the foundation for Li-ion device mechanics and processing constraints. In a composite electrode they are the "glue" which creates a unified mass out of free flowing electroactive and conductive carbon particles, while in a separator they electronically isolate and ionically connect the two halves of the cell.

Electrochemical power generation requires facile electrical and ionic access to the active particles, but most polymer binders do not intrinsically provide either of these functions. PVDF, the most commonly used binder, is electrically insulating, but rendered quite conductive by addition of conductive carbons. In contrast, it is always scarcely ionically conducting since it does not gel in battery electrolytes. (the lowest crystallinity PVDF (a copolymer) had the best conductivity, which was $\sim 1 \times 10^{-5}\,S\,cm^{-1}$ when saturated in a 1 M $LiPF_6$ EC/DEC solution [1]) At these low conductivities, PVDF should be considered to be "Li^+ blocking" rather than "Li^+ transporting". As such, PVDF-based composite electrodes must be porous to allow *liquid* electrolyte to transport Li^+ to the active sites. Towards this goal, a typical composite formulation has much less than 10% binder in order to maintain the electrode porosity. (Without binder, the porosity of an active film is determined primarily by the distribution of sizes and shapes of its particles. For this particular $LiCoO_2$, that value is ~45% porous, or 55% of the density of the pure crystal.) The key to balancing transport and mechanical properties then will be the balancing of the funda-

* Corresponding author.
E-mail address: sjbabinec@dow.com (S. Babinec).

0378-7753/$ – see front matter © 2007 Published by Elsevier B.V.
doi:10.1016/j.jpowsour.2007.06.071

mental transport/strength requirements of porous structures, the need for which originates in the poor Li^+ transport properties of PVDF [1].

2. Experimental

2.1. Electrochemical testing

Composite cathodes were prepared from $LiCoO_2$ particles with ~2–4 μm size (LICO L032) as the active material, and Super-P carbon black as the electronically conductive additive. Both $LiCoO_2$ and carbon black were dried at 120 °C in vacuum oven for 2 h before use. PVDF binder solution (8 wt% in NMP) was supplied by Kruha Co. (7208) and used as received. The cathode slurry was prepared by first mixing $LiCoO_2$ and carbon black particles in a SpeedMixer™ at 2000 rpm for 1 min, adding the binder solution, and then mixing at 2000 rpm for another 5 min. Cathode films of several thicknesses were cast from this *freshly prepared* slurry onto a 25 μm-thick aluminum foil using a Gardco™ draw-down machine with a doctor blade. Wet films were dried in dynamic vacuum at 80 °C for at least 2 h before any measurement or further treatment. These films were often calendared with a single speed two-roll mill (N. Ferrara Inc.). If calendaring is needed, the target thickness (t_t) was calculated from the starting porosity (p_0), thickness (t_0) and the desired porosity (p_t): $t_t = t_0(1-p_0)/(1-p_t)$. Cathode thin film porosity was estimated via a gravimetric method. Specifically, density of a cathode film, d_m, was determined from measuring the weight and thickness of a disk of the cathode film with known diameter (generally 1.27 cm). Porosity, p, of the cathode was then given by $p = 1 - d_m/d_{th}$. The theoretical density, d_{th}, of close-packed cathode materials was calculated according to the relationships: $1/d_{th} = \sum_i \phi_i/d_i$, where ϕ_i and d_i were weight fraction and density of the ith component in the cathode composition, respectively. A density value of 5.10 g cm^{-3} was used for $LiCoO_2$, 1.77 g cm^{-3} for PVDF and 1.90 g cm^{-3} for carbon black.

Electrochemical impedance spectroscopy (EIS) with a Solatron 1480 MultiStat, a Solatron 1255 Frequency Response Analyzer, and Z-Plot/Z-View software package (Scribner Associates) was used to evaluate film electrical and ionic properties. Data was collected in a frequency range of 1–100 kHz, with typical ac amplitudes of 10 mV.

Battery performance testing was via 2025 button cells constructed from amply dried materials in an Argon glove box. Anodes were prepared from MCMB graphites, and had at least twice the mAh capacity as the given cathode. A porous tri-layer PP/PE/PP thin film from Celgard Inc. (2325) was used as the separator and 1 M $LiPF_6$ solution in EC/DEC (1:1) was used as the liquid electrolyte. The same Solatron system described above also ran the battery cycling tests of the button cells using CWare/CView software package (Scribner Associates). A typical charge/discharge testing protocol includes two C/10 charge/discharge cycles and five each of C/2, 1C, 2C, 4C, 6C, 8C, 10C, 15C and 20C charge/discharge cycles with a 5 min open circuit interval between each charge/discharge cycle. The C-rate of button cells was determined based on a theoretical specific capacity 140 mAh g^{-1} for $LiCoO_2$ [2]. Voltage cut-offs are 2.5 V and 4.2 V.

2.2. Mechanical testing

Dense composites of PVDF binders and $LiCoO_2$ particles were prepared by melt blending at 50 rpm and 170 °C using a Haake blender with a 30 ml bowl which was about 2/3 full. The blending was deemed complete upon reaching a constant driving torque, which generally occurred within 10 min. The blends were next compression molded into plates at 170 °C and 20 tonnes of force, using a 7.6 cm × 5.1 cm × 0.08 cm stainless steel chase. Tensile mechanical tests were done on an Instron 4201 frame at a strain rate of 5% min^{-1}, according to ASTM D 882 method.

Instrumented indentation testing (IIT) of composite films was done on a Hysitron TriboScope machine with Berkovich indenter. On every sample, 10 quasi-static (open loop) indentations were done at a 10 μm separation distance. Each indentation test includes a cycle of load (25 s)–hold (10 s)–unload (25 s). The loading/unloading rate was 20 μN s^{-1}, and thus a maximum load of 500 μN was applied. Results were analyzed according to published methods [3].

3. Results and discussion

3.1. Electrochemical and structural characterization

3.1.1. Effect of PVDF content and electrode calendaring on rate capabilities

As described above, porosity is a key cathode composite design parameter since the PVDF solid binder has poor Li^+ conductivity and will block ionic access to the active particle. This variable is therefore examined in some detail. Fig. 1 is battery capacity normalized to the C/10 experimental value versus C-rate for button cell batteries having ~0.7 mAh cm^{-2} cathodes which were prepared using 5–40% binder loading, which shows a pronounced decrease in rate capabilities with increasing PVDF loading. (These cathodes were all calendared to ensure that samples having the best possible performances

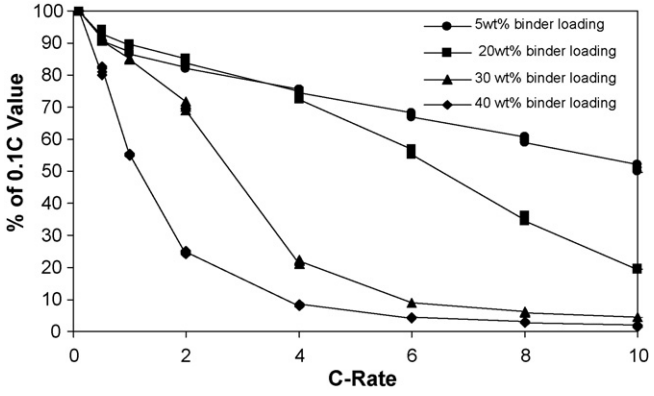

Fig. 1. Discharge capacity (normalized to the 0.1C experimental value) for batteries having 0.7 mAh cm^{-2} capacity cathodes with PVDF binder loading levels of 5%, 20%, 30%, or 40%.

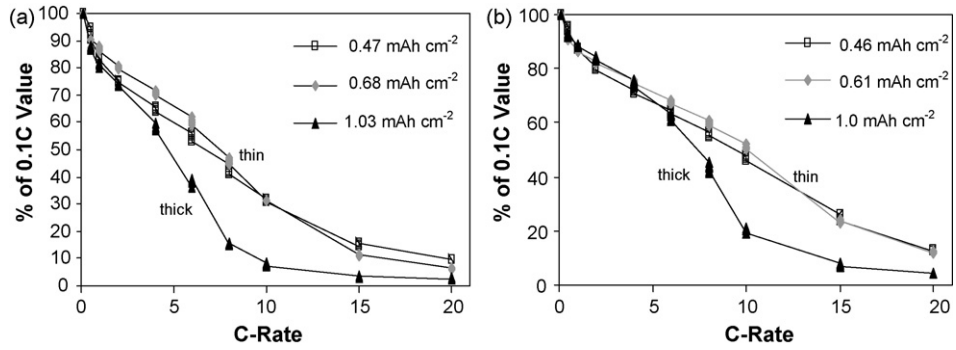

Fig. 2. Normalized discharge capacity vs. C-rate for electrodes of various thicknesses and PVDF content: (a) 5% PVDF—not calendared; (b) 5% PVDF—calendared.

were used for the comparison.) Fig. 2a and b expand upon this theme, and highlight the impact of electrode thickness and calendaring on the battery capacity/C-rate relationship: high rate capabilities are found with thinner cathodes and lower binder loadings. The losses are less severe when the electrodes are calendared.

3.1.2. Effect of PVDF loading and calendaring on microstructure and porosity

Fig. 3a and b shows SEMs of the composite electrode surfaces and shows a quite nonuniform dispersion, with exceptionally large regions of pure PVDF and agglomerated particles. This nonuniformity is related to the rapid evaporation of the sol-

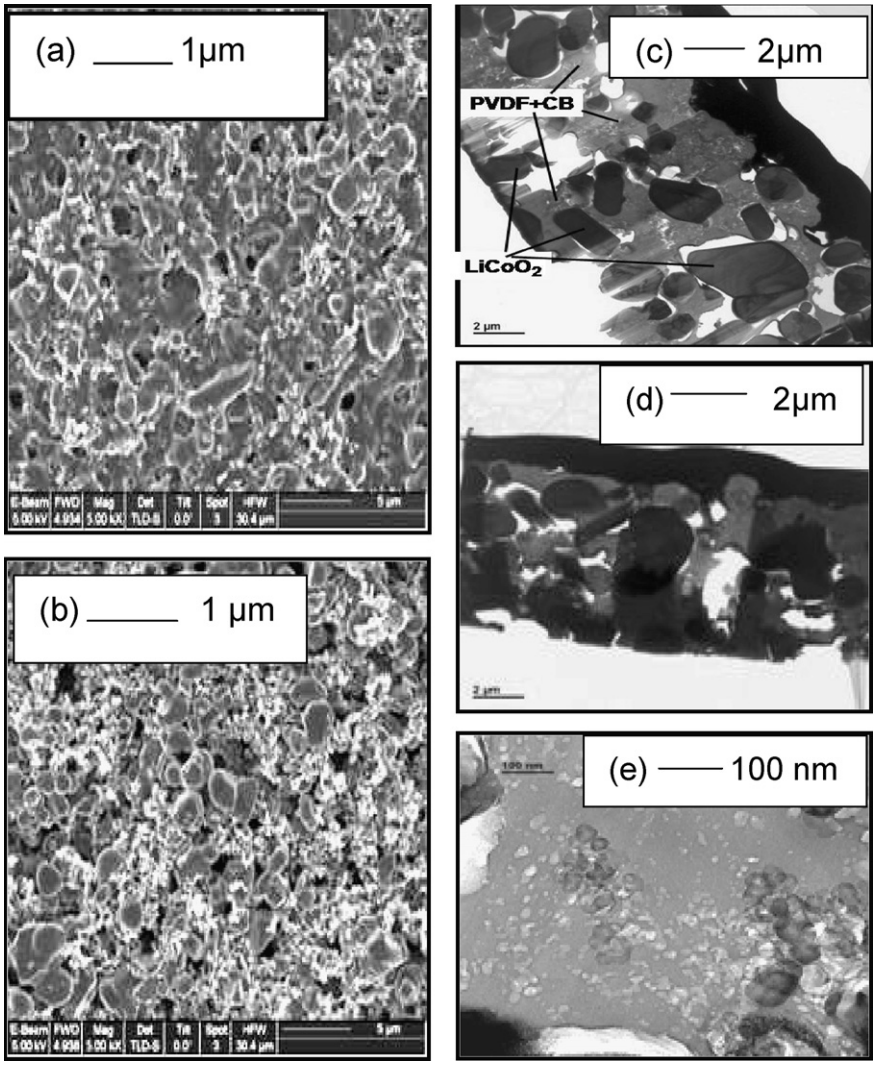

Fig. 3. SEMs of cathode surface for (a) 20% PVDF, and (b) 5% PVDF composite electrodes. TEMs show the microstructure of 20% PVDF composites in detail: (c) uncalendared and (d) calendared electrodes. (e) TEM shows that conductive carbon (small particles) resides nearly exclusively in the PVDF phase.

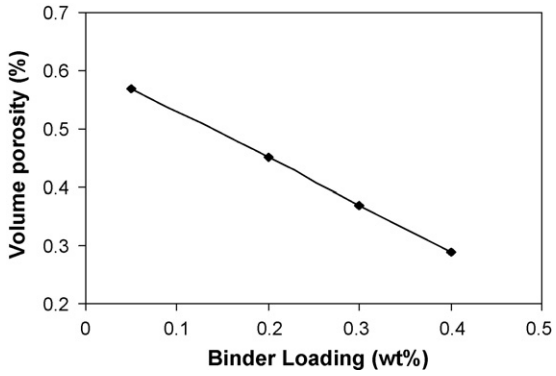

Fig. 4. Composite porosity vs. PVDF binder loading.

vent, providing fast kinetics for PVDF phase separation (from the solvent) which results in random distribution of polymer micro-droplets on the surface. This process does not allow for thermodynamically controlled structures since it is nonequilibrium [4]. Fig. 3c and d shows TEM cross-sections which shows many large gaps, which may be related to poor adhesion between the high surface energy oxide $LiCoO_2$ and low surface energy polymer PVDF. XPS of these samples shows very little difference between pure PVDF and PVDF with $LiCoO_2$, which also indicates little particle/binder interaction. Calendaring densifies the solid and decreases the total porosity, with small cracks remaining at many of the interfaces. If connected to the bulk porosity, these small pores allow liquid electrolyte access to the active particle. However, their limited size and the overall tortuousity of the composite path(s) could also be expected to result in transport limitations at high currents. Fig. 3e shows that the conductive carbons localize in the PVDF matrix, with poor dispersion. The combination of conductive carbon localization in PVDF and poor PVDF/$LiCoO_2$ adhesion can potentially contribute to e^- transport limitations in this complex structure.

Fig. 4 provides quantitative values for bulk porosity of these uncalendared electrodes. As PVDF loading increases, the porosity decreases as expected, with a quite linear relationship in this regime. Fig. 5 is the same data from Figs. 1 and 4 plotted as normalized capacity versus cathode composite porosity,

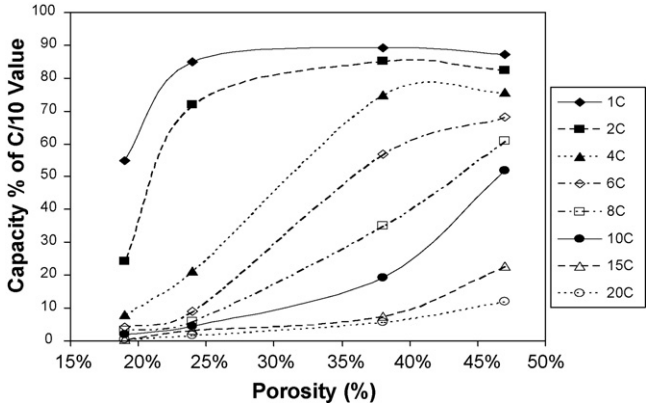

Fig. 5. Normalized capacity vs. composite cathode porosity, with tie-lines of various C-rates.

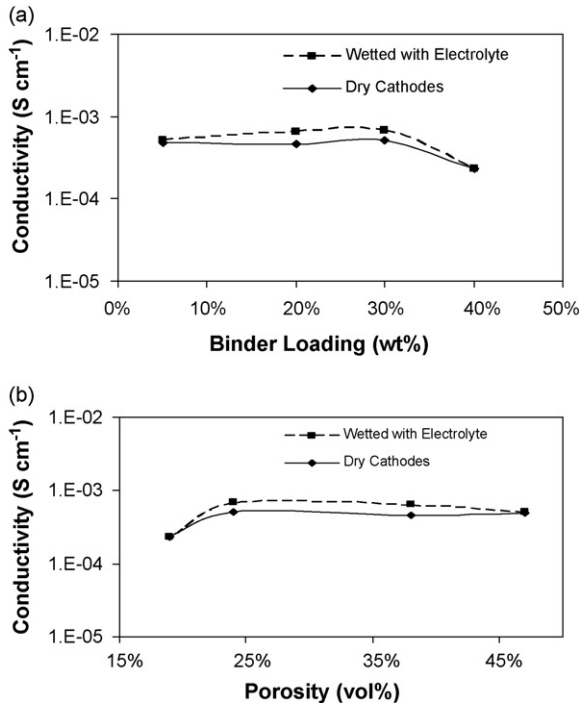

Fig. 6. Electrical conductivity of electrodes vs. (a) PVDF loading and (b) composite porosity.

with tie lines at various C-rates. This plot demonstrates that the decreased total porosity (increased PVDF content) results in decreased electrochemical capacity, and that the effects are largest at high C-rates where transport demands are the greatest. At very low C-rates, which have relaxed transport requirements,

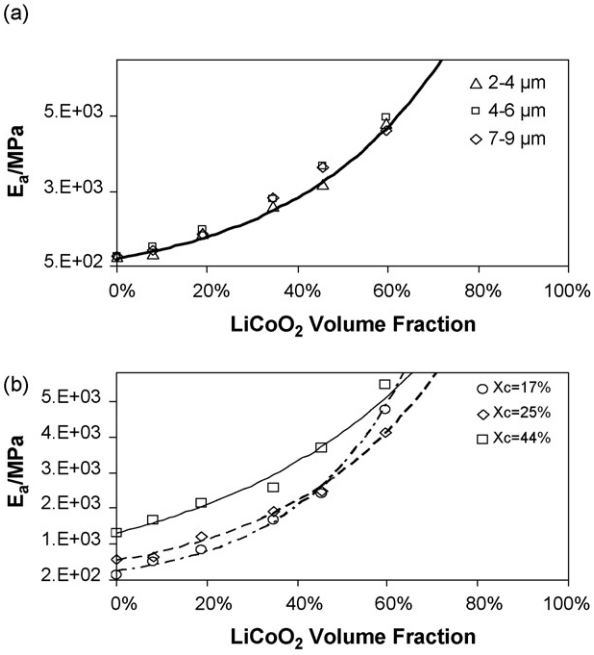

Fig. 7. (a) Elastic modulus vs. $LiCoO_2$ volume fraction in 25% crystalline PVDF for three particle sizes—with comparison to Van der Poel theoretical prediction (solid line). (b) Elastic modulus vs. $LiCoO_2$ volume fraction in PVDF for a 2–4 μm-sized particle in PVDF binders having 17%, 25%, and 44% crystallinity.

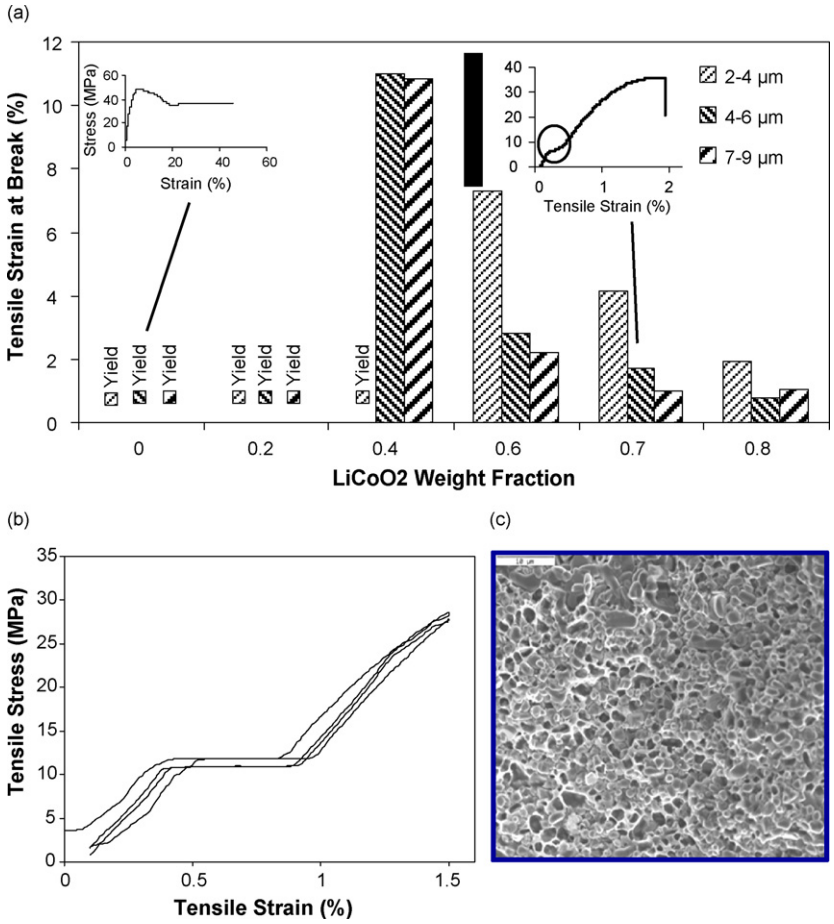

Fig. 8. (a) Tensile strain at break (%) for composites with 25% crystallinity PVDF and $LiCoO_2$ of variable particle size. (b) Cyclic loading of the 70% $LiCoO_2$/PVDF composite in the low strain regime—less than 2%. (c) Secondary electron SEM of fractured surface of (b) showing that particles pull-out of the PVDF at tensile strain of <2%.

porosity does not result in significantly reduced performance until about 20% porosity (40% PVDF loading).

While performance versus porosity can be explained as Li^+ transport issues, e^- transport is another important consideration, since e^- conductivity of the binder can be expected to change with PVDF loading—at constant carbon content. General percolation theory predicts a rapid rise in composite electrical conductivity at ~16–20% volume loading when mixing is statistically random. At this threshold the conductivity changes by approximately 3–6 orders of magnitude, with the inflection point having $\sim 10^{-4}$ S cm^{-1} conductivity [5]. For our composite electrodes, percolation theory predicts the conductivity threshold occurs with PVDF loading of ~18 wt% (5% carbon loading). Thus, higher PVDF loadings should dilute the carbon and ultimately render the blend nonconductive. Fig. 6 shows that theory and experiment do not agree—electrical conductivity (measured by ACI on the dry electrode) is nearly constant from 5% to 30% PVDF, and just begins to drop off at 40% PVDF. Reconsideration of the poor dispersion of carbon in PVDF, as in Fig. 3e, suggests that carbon's nonuniform dispersion in PVDF may be the source of the discrepancy.

Since electrical conductivity is maintained with increasing PVDF loading, poor high rate performance is therefore related to mass transport limitations arising from limited Li^+ access to the active particle in an increasingly nonporous matrix.

3.2. Mechanical characterization of dense composites and porous thin films

3.2.1. Mechanical characterization of dense composites

The first step in our mechanical analysis is to establish whether fully dense $LiCoO_2$/PVDF composites follow expected

Table 1
Modulus and strain at break for solvent swollen PVDF/$LiCoO_2$ composites

$LiCoO_2$ loading in PVDF (%)	Solvent	Solvent load (%)	Young's modulus (MPa)	Strain at break (%)
70	None	0	2700	2.5
70	PC	30	200	15
70	1:1 EC:DEC	30	180	12

Table 2
Young's modulus of dense composites: standard tensile testing of micro-tensile bars and nanoindentation of thin films

$LiCoO_2$ load in PVDF (%)	Solvent	Solvent load (%)	Young's modulus: tensile test (MPa)	Young's modulus: nanoindentation (MPa)
0	None	0	250	1200
20	None	0	710	2400
40	None	0	1000	3300

behaviors, since they can be considered a model of the solid and interfacial regions in the porous composite. Towards this goal, $LiCoO_2$ of three particle sizes (2–4 μm, 4–6 μm, and 7–9 μm) were melt blended with PVDF of variable crystalline content at several loading levels. Fig. 7a is the plot of elastic modulus versus particle volume fraction for the 25% crystalline PVDF and shows a modulus increase with increasing particle loading, which is independent of particle size in this size regime. This behavior is in agreement with theory as described by Van der Poel [6]. Fig. 7b is the same comparison but focuses on the effect of variable crystallinity of the PVDF binder, when $LiCoO_2$ particles are 2–4 μm. Again, there is excellent agreement with theory as the data shows that increases in modulus are largest for the softest binders having the lowest crystallinity. Thus the constituent materials follow expected mechanical behaviors.

Fig. 8a–c shows that the fully dense composites are all relatively brittle: (a) offers the tensile strain at break for composites of moderate crystallinity PVDF and variable size $LiCoO_2$. The composites are ductile below approximately 40% active particle loading, but beyond this show very brittle behavior with strain at break of <10% in the best case scenario. Smaller particles generally provide more ductile ("yielding") behavior, but this advantage is lost with increased loading. At the loading levels used in composite electrodes (~80%), the composites break at less than 2% strain. There is a kink in the stress/strain curve (inset), which is explored in more detail in a separate experiment. Fig. 8b shows the result of exploration of the low strain region for a 70% composite of 2–4 μm-sized particles. During cyclic loading between 0% and 1.5% strain, there is a plateau region, which is characteristic of particle delamination from a matrix, as a mechanism for stress relief. Fig. 8c is the secondary electron SEM micrograph of a fractured surface of this composite, showing extensive particle/matrix delamination. Thus we see that fully dense PVDF/$LiCoO_2$ matrixes are not only brittle, but also fail by particle/matrix delamination. This type of behavior would result in poor composite physical integrity in situations in which the electrode is subjected to these low strains—for example in electrode wind-up or battery sealing operations.

Table 1 compares properties of the dry samples to solvent swollen composites, the latter of which would represent their properties when used in a liquid electrolyte filled battery. The electrolyte-swollen composites have a larger strain at break in comparison to the dry samples, but also suffer brittle failure.

Thin film mechanics are the final step in correlating electrochemical and mechanical performance. Table 2 compares the Young's modulus of fully dense composites measured by standard tensile testing of micro-tensile bars and by nanoindentation of 800 μm thin films of the same fully dense material. It can be seen that nanoindentation consistently provides a modulus more than three times that of the dogbone tensile test. An offsetting of values is not surprising considering that nanoindentation is a compressive test while Young's values are tensile stiffness. Nanoindentation can therefore be considered quite valid for comparison between such films.

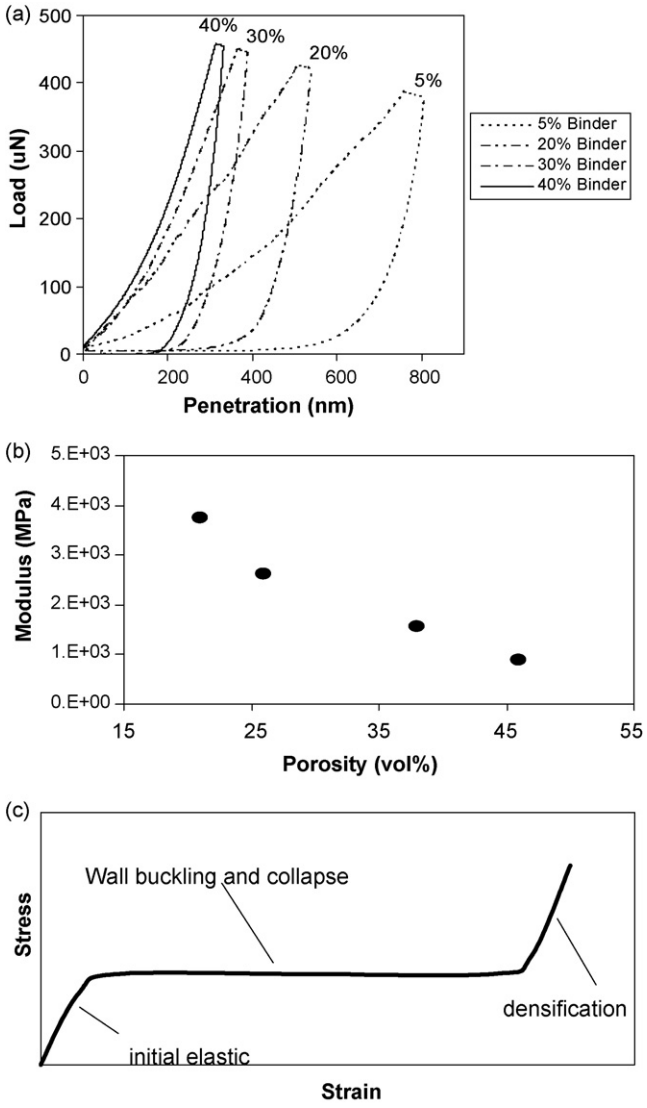

Fig. 9. (a) Load vs. displacement curves for porous thin film composite electrodes of variable binder loading level; (b) modulus as determined in (a) vs. % porosity of composite electrodes; (c) idealized diagram of stress/strain behavior illustrating the collapsing of porous composite walls as the film is put into compression.

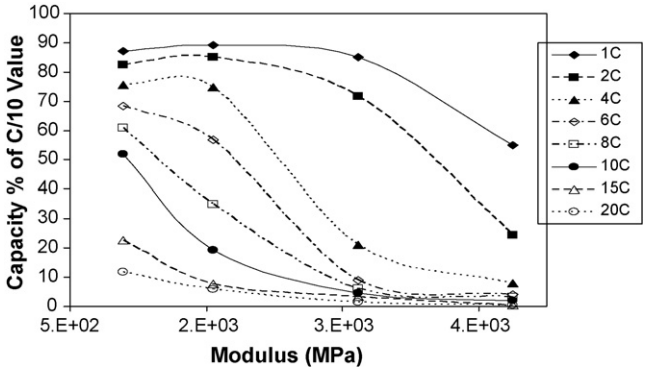

Fig. 10. Electrochemical capacity (normalized to C/10) vs. modulus of composite electrodes having porosity and modulus varied by adjusting the PVDF content.

3.2.2. *Thin porous film mechanics*

Fig. 9a shows the load versus displacement curves for porous thin film composite electrodes of variable binder loading level (films have been calendared). Fig. 9b offers the modulus as determined in (a) but plotted this time versus porosity, which correlates directly with the PVDF loading. The modulus drops by about five times from the least to the most porous of these samples. Equally important however, is that the compressive failure mechanism is a buckling collapse of the porous structure followed by densification, as idealized in the diagram of Fig. 9c. Thus, compression of electrodes during sealing of a battery would be expected to densify the porous structure, which would reduce porosity and negatively effect mass transport.

Fig. 10 plots the electrochemical property of capacity retention versus the mechanical property of modulus as determined by nanoindentation of porous composite electrodes, with tie lines of various C-rates. There is a relatively smooth loss in electrochemical performance as the composite electrode modulus increases. As described above, poor electrochemical performance correlates with low porosity and poor mechanical integrity correlates with both the brittle behavior of composites (illustrated in traditional analysis of dense composites) and with increasing porosity since these porous structures collapse rather than yield under even very small forces. Thus it can be seen that formulations which lead to composite microstructures that provide electrochemically robust performance will also unfortunately result in poor mechanical integrity. This trade-off originates in the need to provide ready Li^+ access to active particles in a matrix based on Li^+ blocking binders that are brittle.

4. Summary

Quite basic studies were offered the effects of formulation on electrochemical and mechanical properties of PVDF/$LiCoO_2$ composite cathodes for Li-ion batteries, focusing on effects of porosity and microscopic structure. As the loading of binder increases, both the porosity and the electrochemical power capabilities decrease. ACI shows that the electrical conductivity of the network remains unchanged and SEM/TEM show the narrowing of pores, in addition to the decrease in total porosity. It is therefore suggested that the loss of power capabilities with increased %PVDF is due to increased Li^+ mass transport limitations. Nanoindentation of porous composite electrodes showed improved mechanical strength with increased binder content, but with a tendency for pores to collapse in all cases, even under very mild compression. Mechanical evaluations of fully dense PVDF/$LiCoO_2$ composites show them to be very brittle, with poor particle/binder interfacial adhesion. In fact, cyclic loading experiments show that $LiCoO_2$ is expelled from the binder under strains as low as 1%. Thus, composite electrode designs which optimize mechanical durability and ruggedness degrade electrochemical performance, due to the requirement for a highly porous structure which optimizes Li^+ transport when crystalline PVDF is used as the binder.

References

[1] M. Watanabe, M. Kanba, H. Matsuda, K. Tsunemi, Makromol. Chem., Rapid Commun. 2 (1981) 741–744.
[2] B. Park, Y.J. Kim, J. Cho, in: G.-A. Nazri, G. Pistoia (Eds.), Lithium Batteries–Science and Technology, Kluwer Academic Publishers, 2004, p. 410 (Chapter 14).
[3] W.C. Oliver, G.M. Pharr, J. Mater. Res. 7 (1992) 1564.
[4] J. Newman, K.E. Thomas-Alyea, Electrochemical Systems, 3rd ed., John Wiley & Sons Inc., Hoboken, New Jersey, 2004 (Chapter 22).
[5] S. Kirkpatrick, Rev. Mod. Phys. 45 (1973) 574.
[6] C. van der Poel, Rheol. Acta 1 (1958) 198–205.